Novel Sample Modulation Device for Flame Spectrometry and Evaluation of Its Utility for Noise Reduction

Momir Marinković[1] and T. J. Vickers

Department of Chemistry, Florida State University, Tallahassee, Fla. 32306

A novel aerosol modulation-slot burner is described, and its performance evaluated. With this device, a hydrogen-air diffusion flame is produced and modulation is accomplished by switching of the aerosol stream by an auxiliary air stream at right angles. The present device is limited to hydrogen-air flames. It is shown that almost complete modulation can be achieved, and that complete suppression of the signal due to background emission can be obtained. Data are presented on the use of this device for atomic absorption measurements with both continuum and line sources, and sample modulation is compared with dc and light chopping modulation techniques with regard to minimization of noise in flame spectrometric measurements.

IN THE SAMPLE MODULATION TECHNIQUE, the supply of sample to the flame is caused to vary in a periodic fashion and the signal information, in either emission or absorption, appears at the modulation frequency. In the present work, we describe a novel sample modulation system in which a slot burner is used and the modulation is accomplished by switching of the sample aerosol stream (*1*). At present this system is limited to H_2-air flames. Sample modulation techniques have been described in a number of papers, only the most recent of which will be cited (*2–6*), and each of these has included some discussion of the merits of sample modulation compared to other measurement techniques. A rather complete list of such advantages has been given, for example, by Herrmann, Lang, and Rüdiger (*7*). Although we have undertaken to examine the performance of the aerosol modulation-slot burner system with respect to such points as the suppression of the background flame emission signal, the aspect of greatest interest to us has been the potential of sample modulation for the improvement of signal-to-noise ratio in flame spectrometric measurements by suppression of low frequency noise components. This aspect does not appear to have been treated in detail previously. In this paper we compare sample modulation with dc and light chopping modulation techniques with regard to optimization of signal-to-noise ratio.

EXPERIMENTAL

The sample modulation-burner system is shown in cross-section and top-view in Figures 1*a* and 1*b*. An H_2-air diffusion flame, 5, is produced above the 0.7- × 40-mm slot. With air as the nebulizing gas, the aerosol is produced in a 130-ml glass chamber (not shown) by a standard Techtron nebulizer and is introduced into chamber 1 of the burner. In the absence of a horizontal air stream, the aerosol is carried through the vertical slot and into the flame, 5. Hydrogen is supplied through the chambers, 4, which run the length of the burner on either side of the vertical slot. Hydrogen enters the flame through a row of 28 evenly spaced holes on each side of the slot, as shown in Figure 1*b*.

An auxiliary air stream is introduced into chamber 2 and exits through the horizontal slot (0.5- × 40-mm). A rotating cylindrical chopper, 3, controls the entry of the air stream into the horizontal channel of the burner. In the present version, the chopper has 10 slots and is rotated by a synchronous motor at 4 revolutions per second. Thus the horizontal air stream is interrupted with a frequency of 40 Hz. Figure 1*c* shows the paths of the vertical and horizontal air streams for the "open" and "closed" positions of the chopper.

With the exception of the chopper, which is made of aluminum, the entire sample modulation burner unit is made of brass and is readily disassembled for cleaning. The internal volume of the horizontal and vertical slots is small in order to allow high modulation frequency. In operation, the whole burner assembly becomes hot, minimizing deposition of aerosol droplets in the chambers and slots and allowing long operation without disassembly for cleaning. Since H_2 and air are not mixed within the burner, the high operating temperature does not present any particular hazard.

The remainder of the equipment employed in the flame emission and absorption measurements is described in Table I. The reference signal to the lock-in amplifier was obtained by modulation of the light incident on a photoconductivity cell with a flat mechanical chopper which had the same number of openings as the cylindrical chopper and was rotated on the same shaft.

RESULTS AND DISCUSSION

Modulation Efficiency. In order to test the efficiency of the auxiliary (horizontal) air stream in "switching" the aerosol stream, the measurements shown in Figure 2 were made. To make these measurements, the cylindrical chopper was removed and the emission intensity was measured as a function of the flow rate of the auxiliary air stream. Conventional light chopping at 40 Hz was employed. The flow rate of the aerosol stream was kept at 8 l./min. The Ni concentration was adjusted to give a signal of approximately the same magnitude as the OH, and OH measurements were made with Ni solution aspirated.

The shape of the curve for Ni 305.76 nm can be explained in the following fashion. With no auxiliary stream input, almost all the aerosol of the vertical stream enters the flame. A weak auxiliary stream bends the aerosol stream and causes a splitting of the stream so that a portion of the aerosol is directed out the horizontal channel. As the flow rate of the auxiliary stream increases, the fraction of the aerosol directed out the horizontal channel increases until the intensity of the Ni line reaches its minimum value at an auxiliary stream flow rate of approximately 9 l./min. At auxiliary stream flow rates

[1] On leave from the Boris Kidrič Institute of Nuclear Sciences, Belgrade, Yugoslavia.

(1) A. Antic-Jovanović, V. Bojović, and M. Marinković, *Spectrochim. Acta, Part B*, in press.
(2) K. Rüdiger, B. Gutsche, H. Kirchhof, and R. Herrmann, *Analyst (London)*, **94**, 204 (1969).
(3) W. Trampisch and R. Herrmann, *Spectrochim. Acta, Part B*, **24**, 215 (1969).
(4) W. Neu, R. Herrmann, and H. Kirchhof, *Messtechnik*, **7**, 154 (1968).
(5) W. Lang, *Spectrochim. Acta, Part A*, **23**, 471 (1967).
(6) W. Lang, *Z. Anal. Chem.*, **219**, 321 (1966).
(7) R. Herrmann, W. Lang, and K. Rüdiger, *Z. Anal. Chem.*, **206**, 241 (1964).

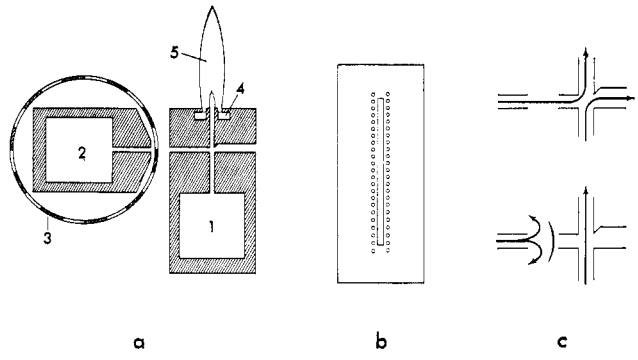

Figure 1. *a.* **Cross-section view of the aerosol modulation–slot burner**

(1) vertical air stream chamber, (2) horizontal air stream chamber, (3) chopper, (4) hydrogen chamber, (5) H_2-air diffusion flame; *b.* top view of burner head showing air slot and holes for entry of H_2 into flame; *c.* diagram of paths of air streams for "open" and "closed" positions of chopper

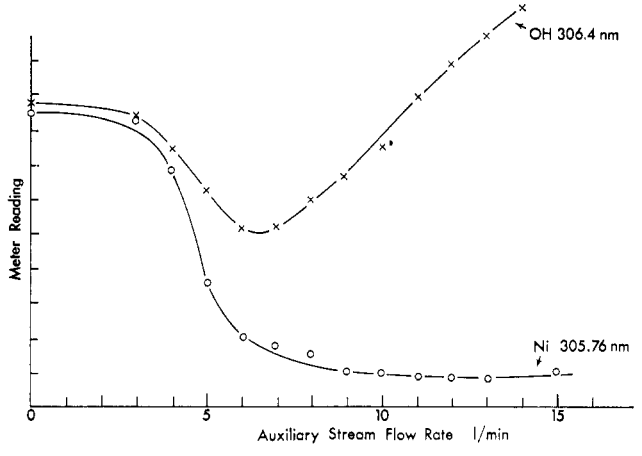

Figure 2. Dependence of the intensities of OH 306.4 and Ni 305.76 nm lines on the flow rate of the auxiliary stream

Aerosol supplied at a constant rate, Ni solution aspirated during OH measurements

Table I. Experimental Apparatus

Spectrometer	Jarrell-Ash model 78-462, 1.0-m Czerny-Turner mount scanning spectrometer with 1180 grooves/mm grating blazed for 5000 Å, curved unilateral slits
Detector	HTV R212, HTV R166 for As measurements
Amplifier	PAR HR-8 lock-in amplifier
Recorder	1-mA galvanometric
Primary sources for absorption measurements	Hollow cathode discharge tubes, tungsten ribbon lamp (GE 30A/T24/17), xenon arc lamp (Hanovia 150 W)

of 9 l./min or greater the Ni emission intensity is less than 10% of its maximum value. The remaining Ni emission is largely due to imperfections in the slots, especially at the ends, a condition which we hope will be remedied in future burners.

The behavior of the OH emission further clarifies the switching action of the auxiliary stream. A weak auxiliary stream appears to cause splitting of the aerosol stream such that the total air flow into the flame (auxiliary plus fraction of aerosol stream) is smaller than that of the undisturbed aerosol stream. For our flame conditions, this will lower the flame temperature and consequently decrease the intensity of OH emission. The concentration of OH must also vary as the

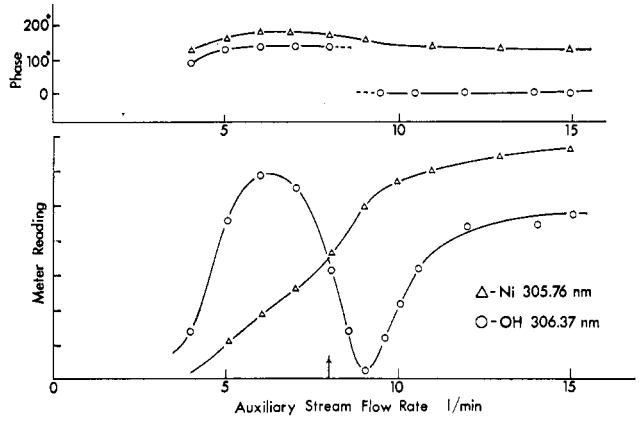

Figure 3. Intensity and phase of OH 306.4 and Ni 305.76 nm lines as a function of the flow rate of the auxiliary stream

Auxiliary stream chopped by rotating cylindrical chopper, Ni solution aspirated during OH measurements

H_2/O_2 ratio varies, and this also will contribute to the change in OH emission intensity. As the auxiliary stream flow rate increases, the OH emission intensity decreases, reaching a minimum at approximately 6 l./min. For auxiliary stream flow rates in excess of 6 l./min the total air flow into the flame apparently increases as the flow rate increases, and finally the OH emission intensity exceeds that seen with no auxiliary stream.

Figure 3 shows measurements of the OH and Ni emission signals with sample modulation employed. To obtain these measurements the cylindrical chopper was placed in position as shown in Figure 1*a*, and the lock-in amplifier was tuned to the modulation frequency. By use of the phase control of the lock-in amplifier, it was possible to determine the phase of the emission signal with respect to the reference signal.

The Ni emission signal first became observable for an auxiliary stream flow rate of about 4 l./min. Apparently appreciable modulation of the sample aerosol stream does not occur at lesser flow rates, as one would anticipate from the results shown in Figure 2. The Ni emission signal increases sharply as the flow rate increases up to approximately 9 l./min at which point the maximum depth of modulation is obtained. Only a small further increase in signal is obtained with a further increase in auxiliary stream flow rate.

The OH emission signal shows a maximum at a flow rate of 6 l./min and a minimum at a flow rate of 9 l./min. These results are in agreement with the measurements reported in Figure 2, since the maximum modulation corresponds to the minimum of Figure 2, and the minimum modulation occurs when the OH emission intensity is the same in both half-periods of the modulation cycle.

The phase measurements offer confirmation of the modulation behavior. The Ni signal shows some small dependence on the auxiliary stream flow rate, but the OH signal shows a sudden change in phase at about 9 l./min, as would be expected from our previous description of the modulation behavior, that is, when the flow rate of the auxiliary stream is less than 9 l./min, the OH emission is more intense when the aerosol stream enters the flame (auxiliary stream diverted by chopper), and when the flow rate is greater than 9 l./min the OH emission is more intense when the auxiliary stream enters the flame. Thus a 180° phase shift is expected in going from less than to more than 9 l./min.

Suppression of Flame Emission Background Signal. The OH curve of Figure 3 is typical of the behavior of all flame

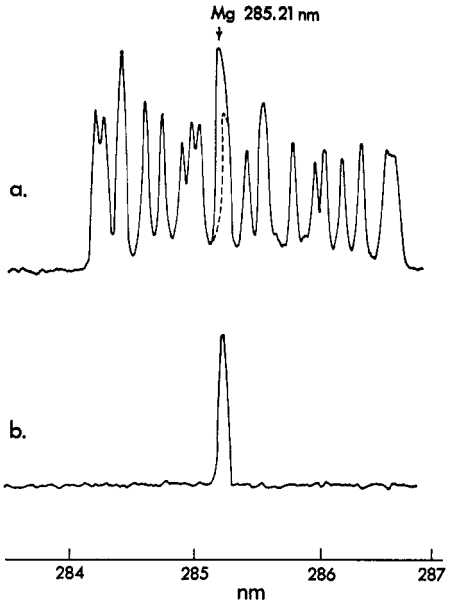

Figure 4. Suppression of OH band signal in the vicinity of Mg 285.2 nm line, 12 ppm Mg

a. **Steady supply of aerosol.** *b.* **Modulated supply of aerosol**

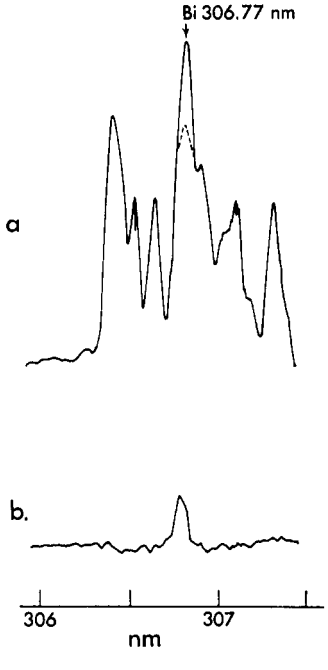

Figure 5. Suppression of OH band signal in the vicinity of Bi 306.7 nm line, 1000 ppm Bi

a. **Steady supply of aerosol.**
b. **Modulated supply of aerosol**

background emission with respect to sample modulation. Elements which are introduced only in the aerosol stream will show the same dependence on auxiliary stream flow rate as Ni. From Figure 3 it may be seen that it is possible to choose an auxiliary stream flow rate at which the flame background emission signal will be very nearly completely eliminated. Figures 4 and 5 show two examples of the suppression of the OH emission signal by sample modulation.

Scanning of Flame Atomic Absorption Spectra. Figure 6 shows a portion of the spectrum of Fe. The top trace of Figure 6 was obtained by conventional (light chopped, constant introduction of Fe aerosol) atomic absorption with a Xe arc continuum primary source. Ten times scale expansion was used. The Fe concentration was 500 ppm.

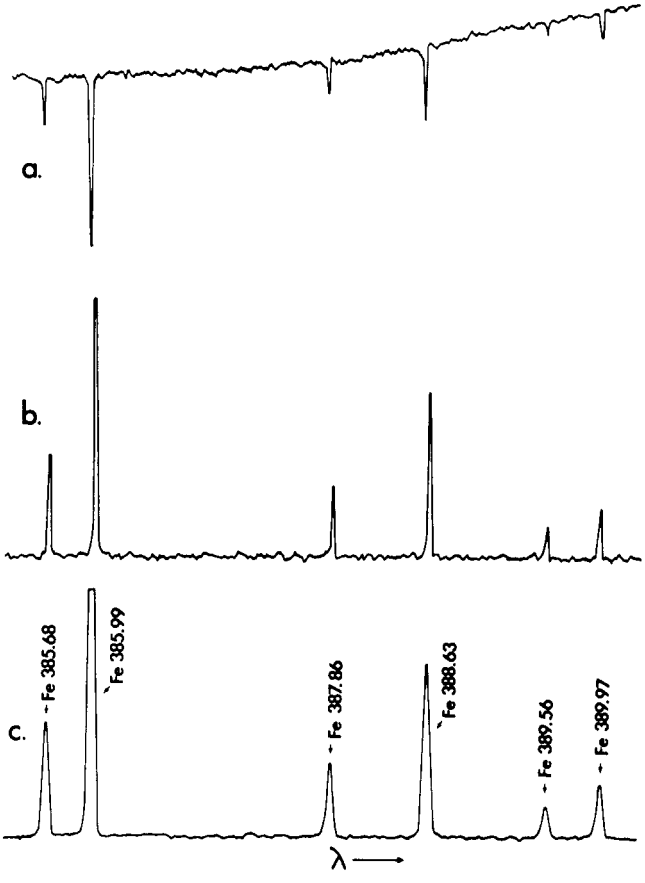

Figure 6. Iron spectrum in the range 385.0 to 390.0 nm, 500 ppm Fe

a. **Absorption, steady supply.** *b.* **Absorption, modulated supply** *c.* **Emission**

The variation of the background curve with wavelength is attributable to the spectral distribution of emission of the Xe lamp, to spectral response of the multiplier phototube detector, and to the intensity drift of the primary source. The middle trace of Figure 6 shows the absorption spectrum obtained with sample modulation. No zero off-set was applied. In this case, the peak heights are proportional to the intensity of absorbed radiation, I_A, where $I_A = I^\circ - I$, and I° is the transmitted intensity in the absence of sample aerosol and I is the transmitted intensity when sample aerosol is introduced to the flame. It should be noted that the base line is flat, indicating that it is not affected by the variation of I°, change in detector response, or source drift. For the sake of comparison, the lower curve gives the Fe emission spectrum. The slightly wider lines are due to the larger slit width employed in this case. It is interesting to note that all the lines which appear in emission also appear in absorption, and that the relative intensities of lines in the emission and absorption spectra are approximately the same.

Analytical Curve for Flame Atomic Absorption. With sample modulation, the absorption signal is directly proportional to the intensity of radiation absorbed, if 100% modulation is assumed, and, for slit widths at which the monochromator band pass is much greater than the width of the absorption line, directly proportional to the monochromator slit width (*8*). The evaluation of the intensity of radiation absorbed for continuum and line sources has recently been

(8) J. D. Winefordner and T. J. Vickers, ANAL. CHEM., **36**, 1939 (1964).

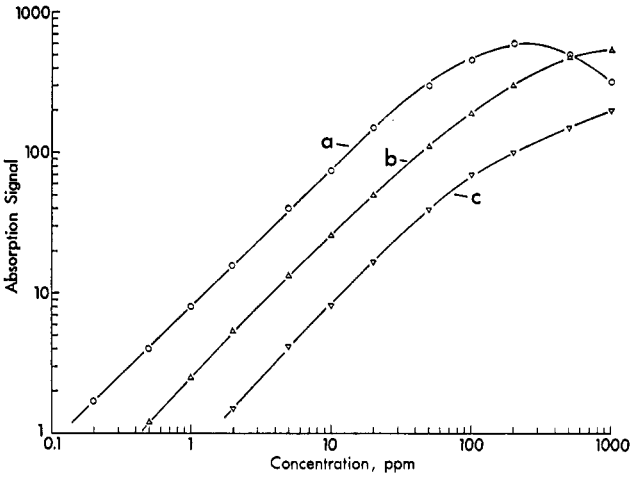

Figure 7. Analytical curves for Cr 425.4-nm line

a. **Hollow cathode tube.** *b.* **Xe lamp.** *c.* **Tungsten lamp**

discussed in some detail (*9*). Applying the results of (*9*) yields for the case of sample modulation with a continuum primary source that the absorption signal at low atomic concentrations is given by

$$S_c = KWI_{\lambda c}{}^{\circ}Nl \qquad (1)$$

where K is a constant, W is the slit width, $I_{\lambda c}{}^{\circ}$ is the intensity of the continuum source at wavelength λ, N is the atomic concentration, and l is the path length through the flame. When a narrow line primary source is employed, the absorption signal is given by

$$S_L = K'WI_LNl \qquad (2)$$

where I_L is the integrated intensity of the emission line.

Equations 1 and 2 indicate that a log-log plot of signal *vs.* concentration is advantageous when sample modulation is used since, for low atomic concentrations, log S = log N + log(source intensity) + log(constant). Thus a log-log plot should give a curve with unity slope. Variation of the source intensity will shift the curve vertically along the signal axis but will not alter the shape of the curve.

Analytical curves for the Cr 425.4-nm line are shown in Figure 7. The slit width for each was chosen on the basis of optimization of the signal-to-noise ratio as described in a subsequent section. The slit widths employed were 400 μm for the hollow cathode source, 30 μm for the Xe source, and 50 μm for the tungsten source. In the low concentration range, the curves all show approximately the predicted unity slope. The negative slope of the hollow cathode curve at very high concentrations is unexpected, since at high concentrations a zero slope should be observed with a line source (*9*). The occurrence of this effect only with the line source suggests that it is due to broadening of the absorption line with consequent reduction of the absorption coefficient at the line center.

Signal-to-Noise Ratio Measurements for Flame Atomic Absorption. Figure 8 shows the results of signal-to-noise ratio measurements carried out on the Cr 425.4-nm line with sample modulation for the three primary sources. Emission from the flame was negligible when the hollow cathode or xenon source was used, but the emission signal was about

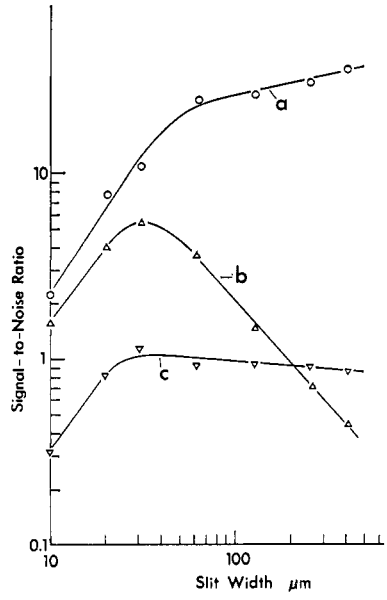

Figure 8. Signal-to-noise ratio as a function of the slit width of the monochromator for atomic absorption at Cr 425.4 nm line, 2 ppm Cr.

a. **Hollow cathode tube.** *b.* **Xe lamp.** *c.* **Tungsten lamp**

0.20 as large as the absorption signal when the tungsten lamp was used. The reported results have been corrected for the flame emission. Since the emission signal is opposite in phase to the absorption signal and, therefore, decreases the measured absorption, correction for emission is easily accomplished by adding the emission signal to the measured absorption. The results shown in Figure 8 are for a solution concentration of 2 ppm of Cr, and the noise was estimated from the width of the recorder trace with all conditions the same as for measurement of the sample absorption signal but only water aspirated. In all measurements, noise from the electronic equipment was found negligible compared to the source and flame noise (shot and flicker). A 1-second time constant was used. The equivalent noise bandwidth, calculated from manufacturer's information, was approximately 0.25 Hz.

The relationship between signal and slit width is given in Equation 1 for a continuum source and in Equation 2 for a line source. By the term noise we mean spurious signal components which may occur at any frequency within the capabilities of the measurement system and which have a random phase relationship with other components of the signal. Because of its random nature, noise can not be dealt with mathematically in the same fashion as coherent signals, but it can be described in terms of its mean square or root-mean-square (RMS) current or voltage values. Noise may arise from several sources: fluctuations in the environment, thermal motion of charges in resistors or other electronic components (Johnson noise), flicker noise ($1/f$ noise) in electronic components, including the detector, flicker noise in light sources and the flame, and shot noise. In flame spectrometry the latter two types are of principal importance, and only these two will be discussed here.

RMS detector shot noise is directly proportional to the square root of the current in the multiplier phototube (*8*). In all of our measurements, dark current made a negligible contribution to the current, and, under these conditions, the

(9) P. J. T. Zeegers, R. Smith, and J. D. Winefordner, ANAL. CHEM., **40** (13), 26A (1968).

Table II. Signal-to-Noise Ratio Expression for Line and Continuum Primary Sources, Dark Current Negligible, $s = R_d W$

	Line	Continuum
Shot noise limited	$K_1 \left(\frac{I_L}{\Delta f}\right)^{1/2} N l W^{1/2}$	$K_2 \left(\frac{I^{\circ}_{\lambda c}}{\Delta f}\right)^{1/2} N l$
Source flicker noise limited	$K_3 \frac{N l}{\Delta f^{1/2}}$	$K_4 \frac{N l}{W \Delta f^{1/2}}$

shot noise depends directly on the square root of the radiant power incident on the photocathode. RMS source flicker noise depends directly on the radiant power from the source incident on the detector (*8*), for a given measurement frequency and frequency response bandwidth of the measurement system. Flame flicker noise shows the same type of dependence. For a continuum source, the incident power increases as $W^2 I_{\lambda c}{}^{\circ}$ for slit widths for which the monochromator band pass is adequately described by $s = R_d W$, where R_d is the reciprocal linear dispersion (*8*). For a line source, the incident power increases as $W I_L$ (*8*).

The signal-to-noise ratio expressions which result in various limiting cases are summarized in Table II. Comparing these expressions with the curves of Figure 8 for which the logarithm of the signal-to-noise ratio has been plotted against the logarithm of the slit width, it is apparent that for large slit widths (>30 μm), the signal-to-noise ratio for the tungsten and hollow cathode sources is largely shot noise limited, and for the Xe arc source is largely source flicker noise limited. At narrow slit widths the signal decreases more rapidly than predicted by Equations 1 and 2, apparently due to aberrations and diffraction effects. Flame flicker noise was found to be small but appreciable. The small negative slope at large slit widths for the tungsten source is due to the flame flicker noise contribution.

Comparison of Modulation Techniques. If one considers the frequency spectrum of the noise types described in the preceding section, it is possible to point out those situations in which sample modulation will lead to an improvement in signal-to-noise ratio as compared to other modulation techniques. Noise, we have said, contributes random, spurious components to the signal, and thus we may view the recorded analog signal as a dc current or voltage with a superimposed random ac noise component. The mean-square noise current is then defined as

$$n^2 = \frac{1}{t}\int_0^t i^2 \mathrm{d}t, \tag{3}$$

where i is the amplitude of the ac component of the analog signal, and t is the measurement time. The measurement time must be large compared to the time constant of the measurement system. By noise spectrum, we mean the variation in amplitude of the RMS noise current or voltage which would be observed as a function of measurement frequency by a measurement system of unit frequency response bandwidth.

The spectra of thermal noise and shot noise are white, that is, of equal amplitude at all frequencies, but flicker noise in electronic components shows approximately a $1/f$ distribution, where f is the frequency (*10*). Source and flame flicker noise similarly shows a much greater amplitude at low frequency

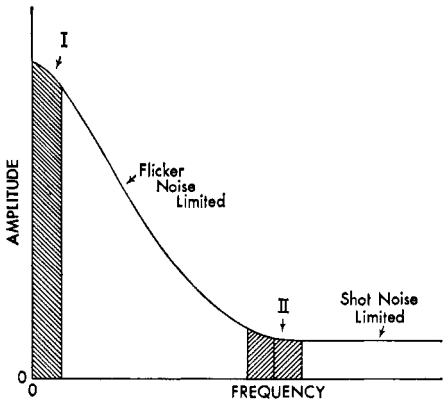

Figure 9. Typical noise spectrum for flame spectrometric measurement with appreciable source flicker

than at high (*11*). Thus for a flame spectrometric measurement in which flicker noise is appreciable, the noise spectrum will have a form such as that shown in Figure 9.

Every real measurement system has a finite frequency response bandwidth, $\Delta f = f_2 - f_1$, where f_2 and f_1 are the upper and lower limits of the band passed. Thus the mean square noise passed by the measurement system is given approximately by

$$n^2 = \int_{f_1}^{f_2} A_f{}^2 \mathrm{d}f \tag{4}$$

where A_f is the amplitude of the RMS noise at frequency f. From the preceding, it may be seen that the total RMS noise which appears in the measurement system output depends on the frequency response bandwidth and, if the noise is not white, on the mean frequency of the band. It is instructive to consider the noise band passed in flame emission and flame absorption measurements with each of the following measurement techniques: dc measurement, ac measurement with light chopping, and ac measurement with sample modulation.

When a dc system is used for flame emission measurements, the information of interest appears at 0 Hz and the width of the noise band passed is determined by the characteristics of the low pass filter. For an RC low pass filter, the equivalent noise bandwidth is given by

$$\Delta f = \frac{1}{4RC}. \tag{5}$$

Thus noise in the interval Δf will be superimposed on the signal of interest. This interval has been designated as region I on Figure 9.

A mechanical chopper placed between flame and monochromator modulates the emission (signal and noise), in effect multiplying it by 1 when in the open position and by 0 when in the closed position. For the purposes of this work we can define the "chopper function" to be periodic and determined as follows: $G_{ch} = 0$ for $0 < t < (\tau/2)$ and $G_{ch} = 1$ for $(\tau/2) < t < \tau$, where τ is the period of chopping and is equal to $1/f_c$ where f_c is the chopping frequency.

If we represent a component of the emission as

$$F_e = A_e \sin(2\pi f_e t) \tag{6}$$

(10) R. R. Benedict, "Electronics for Scientists and Engineers," Prentice-Hall, Englewood Cliffs, N. J., 1967.

(11) Yu. I. Belyaev, L. M. Ivantsov, A. V. Karyakin, P. H. Phi, and V. V. Shemet, *Zh. Anal. Khim.*, **23**, 980 (1968); *J. Anal. Chem. U.S.S.R.*, **23**, 855 (1968).

Table III. Noise of Xe Arc Lamp at Different Frequencies (Δf = 5 Hz)

Frequency, Hz	Noise (% of signal)
"0"	0.87
20	0.18
40	0.09
80	0.04
160	0.04

Table IV. Detection Limits, ppm

		Modulation	
Line, nm	Source	Light	Sample
Ni 232.0	Hollow cathode	0.035	0.019
As 193.6	Electrodeless discharge	9.5	2.8
Cr 425.4	Hollow cathode	...	0.026
Cr 425.4	Xe arc lamp	2.0	0.15
Cr 425.4	W Lamp	...	2.1

where A_e is the amplitude of the component and f_e is the frequency, and if we take only the first two terms of the Fourier series describing the chopper function, then the chopper modulated emission is given by

$$A_e \sin(2\pi f_e t)\left[\frac{1}{2} + \frac{2}{\pi}\sin(2\pi f_c t)\right] = \frac{A_e}{2}\sin(2\pi f_e t) + \frac{A_e}{\pi}\cos\{[2\pi t(f_c - f_e)] - \cos[2\pi t(f_c + f_e)]\}. \quad (7)$$

From Equation 7 it can be seen that the information which originally appeared at f_e now appears at $f_c + f_e$ and $f_c - f_e$. If, as in the usual flame emission case, the information of interest originally appeared at $f_e \simeq 0$, the result of chopping is to cause the information to appear at the chopping frequency, f_c. Noise which originally appeared at frequencies near f_e will as a result of chopping appear in a band symmetrically disposed about f_c. In the usual case the information will then be amplified by an ac amplifier (usually tuned to the chopping frequency but with a broad bandpass), detected (changed from ac to dc), and filtered by a low pass filter. If the low pass filter is identical to that employed in the dc measurement system the noise bandpass remains the same, that is, the noise given by region I of Figure 9, and if flame noise predominates, use of a mechanical chopper and an ac measurement system offers no advantage over the dc system. If the principal source of noise lies in the electronic components in the measurement system, and if the noise spectrum shows a $1/f$ dependence, then the change of signal frequency would be advantageous.

When sample modulation is employed, the information of interest appears at the modulation frequency. If the same ac measurement system described above were employed for the sample modulated signal measurement, a considerable improvement in signal-to-noise ratio could be observed if flame flicker noise predominated since the noise band passed is now that of region II of Figure 9. An improvement of signal-to-noise ratio of as much as a factor of 10 has been observed (*1*). No improvement in signal-to-noise ratio would be expected if the principal noise were white in distribution.

In flame absorption measurements, with which we are principally concerned in this paper, both the primary source and the flame absorption cell can contribute to the total noise. The flame can show a flicker effect due to both its emission and absorption. Although there are additional potential noise sources in flame absorption measurements, in general the arguments developed above for flame emission apply. For a dc measurement system, both source and flame noise lie in region I of Figure 9. When a mechanical chopper is inserted between source and flame and an ac measurement system is used, the source noise is from region I but flame noise is from region II. With sample modulation, both source and flame noise lie in region II. It is interesting to note that with a double beam atomic absorption instrument which uses a mechanical chopper both the source and flame absorption noise will be modulated, and hence both will arise from region I. Note that the frequency shift from region I to region II will only result in an appreciable improvement in signal-to-noise ratio when the noise spectrum is similar to that of Figure 9; if the noise spectrum is white, no appreciable improvement will be observed.

Table III shows the results of noise measurements made with the Xe arc source. With no chopping, the noise was observed with the lock-in amplifier tuned to the noted frequencies. With chopping of the light, the noise passed is assumed, in accordance with the preceding discussion, to arise in the range near zero frequency and is reported in the line labeled "0" Hz.

Detection Limits. Table IV compares the detection limits obtained by the light chopping and sample modulation techniques. Note that a substantial improvement in detection limit is obtained only in the case in which the Xe arc is used as the primary source. This is in agreement with the preceding discussion, since only with the Xe arc did we find source flicker to be the predominant noise source.

CONCLUSIONS

We have demonstrated that the aerosol modulation–slot burner is a practical sample modulation device, but we believe that the most significant aspect of the work reported here is the delineation of the rather limited circumstances in which sample modulation can result in a significant improvement in signal-to-noise ratio compared to a light chopping technique. These circumstances are: the noise spectrum shows an appreciably greater magnitude at low frequency than at the modulation frequency, and the noise is principally determined by source or flame fluctuations.

RECEIVED June 2, 1970. Accepted August 14, 1970. Work supported in part by funds from National Science Foundation Grant GP 7160 and PHS Grant R01GM15996-02 from the National Institute of General Medical Sciences.